

# Thermal decomposition kinetics of aluminum sulfate hydrate

Gülbanu Koyundereli Çılgı · Halil Cetişli

Received: 2 December 2008 / Accepted: 23 July 2009 / Published online: 13 August 2009  
© Akadémiai Kiadó, Budapest, Hungary 2009

**Abstract** The kinetics of individual stages of thermal decomposition of  $\text{Al}_2(\text{SO}_4)_3 \cdot 18\text{H}_2\text{O}$  were studied by TG method. It is found that  $\text{Al}_2(\text{SO}_4)_3 \cdot 18\text{H}_2\text{O}$  decomposes to  $\text{Al}_2\text{O}_3$  in four major stages, all of endothermic. Some of these major stages are formed by sub-stages. The first three major stages are dehydration reactions in which two, ten and six moles water are lost, respectively. The last major stage is sulfate decomposition. In this study the kinetic parameter values of these major and sub-stages were calculated by integral and differential methods. The alterations of activation energies with respect to the decomposition ratio and to the method were investigated.

**Keywords** Thermal decomposition · Aluminum sulfate · Thermogravimetric analysis · Activation energy

## Introduction

The processes which occur during solid decompositions are complex leading to experimental observations which can be very different under even slightly changed conditions. These problems arise from the great variety of possibly uncontrolled systems variables, such as the nature of the solid reactant (single crystal, powder), its pretreatment (grinding, annealing, etc. which influence the defect content and its nature), sample mass or size (which affect mass and energy transfer) and experimental conditions (rate of temperature rise, pressure, nature of the surrounding atmosphere, removal or otherwise evolved gases) [1, 2]. So

it is very difficult to define a single equation for kinetics of thermal decomposition events.

For many decades aluminum sulfate, has been the standard raw material of the water treatment industry. It is large molecular size and weight, combined with low cost, make it an excellent flocculants for the treatment of both drinking water and industrial waste water. In addition to water treatment, aluminum sulfate finds use in a diversity of other areas including construction products, oil and fat processing, and paper manufacturing.

The thermal decomposition of sulfate compounds have been studied for many years [3–6]. Chou and Soong studied thermal decomposition of anhydrous aluminum sulfate and aluminum sulfate hydrate compounds under isothermal and dynamic conditions.

They investigated the effects of various reaction conditions on decomposition kinetic, such as different heating rates and sample weights [7, 8]. But they did not calculate activation energy values and determine reaction models for every decomposition stages.

In this study, the kinetics of thermal decomposition of  $\text{Al}_2(\text{SO}_4)_3 \cdot 18\text{H}_2\text{O}$  compound has been reexamined in detail from a fresh point of view. Activation energies of decomposition stages are calculated via, Ozawa, KAS (Kissinger–Akahira–Sunose), Isoconversional and Friedman model free equations. The alterations of activation energies with respect to the decomposition fraction and to the method were investigated. The reaction enthalpy values of major and sub-stages were calculated with the help of DTA peak areas.

## Thermal decomposition kinetics

The experimental data for the kinetic analysis of heterogeneous solid–gas reactions can be obtained under

G. K. Çılgı (✉) · H. Cetişli  
Department of Chemistry, Faculty of Science and Arts,  
Pamukkale University, 20070 Denizli, Turkey  
e-mail: gkcilgi@gmail.com

different conditions. The non-isothermal thermogravimetry (TG) with a linear temperature growth is a method frequently used to characterize materials from their thermal behavior standpoint. In addition, it enables to determine apparent kinetic parameters of heterogeneous reactions (the reaction order  $n$ , the activation energy  $E$  and the frequency factor  $A$ ). Considerable attention is paid to the kinetic parameters calculation from TG curves. New calculation methods are still being published [9, 10].

We here analyse the data obtained under non-isothermal conditions, with a linear regime of temperature increase in time ( $\beta = dT/dt = \text{const.}$ , where  $\beta$  is the heating rate,  $T$  is the temperature and  $t$  is the time). Under such conditions, for a heterogeneous solid–gas reaction, which occurs in a single stage, the reaction rate is expressed by the well-known general equation:

$$\frac{\partial \alpha}{\partial T} \beta = A e^{-E/RT} f(\alpha) \quad (1)$$

where  $\alpha$  is the degree of conversion,  $A$  is the frequency factor,  $E$  is the activation energy,  $f(\alpha)$  is the differential conversion function and  $R$  is the gas constant. Equation 1 may also lead to the corresponding equations of the Ozawa, KAS, Isoconversional after integration form and Friedman method after logarithmic form [11–23].

Ozawa equation;

$$\ln \beta = \left[ \frac{AE}{Rg(\alpha)} \right] - 5.3305 - 1.05178 \frac{E}{R} \frac{1}{T} \quad (2)$$

For  $\alpha = \text{const.}$ , the plot of  $\ln \beta$  versus  $1/T$ , obtained from curves, which are recorded at several heating rates, should be a straight line with a slope that allows an evaluation of the activation energy.

KAS equation;

$$\ln \frac{\beta}{T^2} = \ln \frac{AR}{g(\alpha)E} - \frac{E}{R} \frac{1}{T} \quad (3)$$

For  $\alpha = \text{const.}$ , the plot of  $\ln \beta/T^2$  versus  $1/T$ , obtained from curves, which are recorded at several heating rates, should be a straight line with slope that allows an evaluation of the activation energy.

Isoconversional equation;

$$-\ln t = \ln \frac{A}{g(\alpha)} - \frac{E_a}{R} \frac{1}{T} \quad (4)$$

For  $\alpha = \text{const.}$ , the plot of  $-\ln t$  versus  $1/T$ , obtained from curves, which are recorded at several heating rates, should be a straight line with a slope that allows an evaluation of the activation energy.

Friedman equation;

$$\ln \frac{\partial \alpha}{\partial t} = \ln \beta \frac{d\alpha}{dT} = \ln Af(\alpha) - \frac{E}{RT} \quad (5)$$

For  $\alpha = \text{const.}$ , the plot of  $\ln d\alpha/dt$  versus  $1/T$ , obtained from curves, which are recorded at several heating rates, should be a straight line with a slope that allows an evaluation of the activation energy.

## Experimental

Aluminum sulfate-18 hydrate was obtained from Aldrich. All of the thermogravimetry (TG), derivative thermogravimetry (DTG) and differential thermal analysis (DTA) curves were obtained simultaneously by using a Shimadzu DTG-60H Thermal Analyzer. The measurements were carried out in a flowing nitrogen atmosphere with a flow rate of 25 mL min<sup>-1</sup> and a temperature ranged from 25 to 1000 °C in an alumina crucible. The heating rate ( $\beta$ ) varied as 8, 6, and 4 °C min<sup>-1</sup>, where the sample mass ( $w_0$ ) was ranged from 10 to 12 mg. All of the experiments were performed twice for repeatability and the results showed good reproducibility with the smaller variations in the kinetic parameters. Finally, highly sintered Al<sub>2</sub>O<sub>3</sub> was used as the reference material.

## Results and discussion

The thermal analysis results from the evaluation of curves obtained at all heating rates are summarized in Table 1. However, only the curve that is obtained at heating rate of 4 °C min<sup>-1</sup> is presented in Fig. 1 as an example. It is found that aluminum sulfate-18 hydrate's decomposition consists of four major steps, all endothermic. Some of these major steps are formed by sub-stages.

The 18 moles of water in the compound leaves the body at three major stages. The peak temperatures for the dehydration reaction at Stage-I and II, and the temperature range for the reaction increase with the increase of heating rate- $\beta$ , which is programmed during the thermal analysis.

While split of the peaks occurs for the first stage (I) dehydration event (320.75 K) and for the second stage (II) dehydration event (336.08 K) at a heating rate of 4 °C min<sup>-1</sup>, the peaks of dehydration reaction for Stage-I and II overlaps at highest heating rate (8 °C min<sup>-1</sup>). If two consecutive physical or chemical events exist, events can be observed as a single event in the curve for higher heating rates. Hence, the dehydration reaction enthalpy of the Stage-I was able to be determined only at lower heating rates. It is proved by the dehydration reaction enthalpy of the Stage-I at lower heating rate (72.93 kJ mol<sup>-1</sup>), which is higher than the evaporation enthalpy of the water (40.60 kJ mol<sup>-1</sup>), that the water molecules chemically bounded to the compound.

**Table 1** The mass loss data for the decomposition of  $Al_2(SO_4)_3 \cdot 18H_2O$  at different heating rates

$\beta/w_0$	Property	Dehydration steps						Sulfate decomposition step			
		DTA-TG-DSC									
		I	II	I + II	IIIa	IIIb	IIIc	III	IVa	IVb	IV
4 °C min <sup>-1</sup> , 10.497 mg	$(T_i - T_f)/K$	325–354	354–437	325–437	437–580	580–640	640–965	437–965	965–1043	1043–1103	965–1124
	$T_{peak}/K$	336.08	397.40	–	561.64	629.77	–	–	1029.14	1091.19	–
	$(w_i - w_f)/mg$	0.567	2.841	3.408	0.850	0.427	0.425	1.702	0.632	2.844	3.659
	$(\Delta w/w_0) \cdot 100$	5.402	27.065	32.466	8.098	4.068	4.049	16.214	6.021	27.093	34.858
	Product mole	2	10	12	3	1.5	1.5	6.0	0.50	2.25	2.90
	$\Delta H/J g^{-1}$	218.88	1120.00	1560.00	–	–	–	–	58.84	356.47	–
6 °C min <sup>-1</sup> , 10.880 mg	$(T_i - T_f)/K$	325–362	362–442	325–442	442–585	585–640	640–972	442–972	972–1043	1043–1110	972–1142
	$T_{peak}/K$	356.25	401.05	–	–	631.17	–	–	1008.77	1101.24	–
	$(w_i - w_f)/mg$	0.590	2.944	3.534	0.885	0.447	0.446	1.778	0.642	2.948	3.788
	$(\Delta w/w_0) \cdot 100$	5.423	27.059	32.482	8.134	4.108	4.099	16.287	6.094	27.040	34.816
	Product mole	2	10	12	3	1.5	1.5	6.0	0.50	2.25	2.90
	$\Delta H/J g^{-1}$	110.18	959.89	1500.00	–	–	–	–	–	144.93	–
8 °C min <sup>-1</sup> , 10.543 mg	$(T_i - T_f)/K$	334–375	375–458	334–458	458–595	595–653	653–980	458–980	980–1050	1050–1117	980–1148
	$T_{peak}/K$	370.18	403.26	–	–	630.42	–	–	–	1110.11	–
	$(w_i - w_f)/mg$	0.570	2.852	3.422	0.858	0.427	0.425	1.710	0.634	2.846	3.670
	$(\Delta w/w_0) \cdot 100$	5.406	27.051	32.458	8.138	4.050	4.031	16.219	6.013	26.994	34.810
	Product mole	2	10	12	3	1.5	1.5	6.0	0.50	2.25	2.90
	$\Delta H/J g^{-1}$	–	–	1490.00	–	–	–	–	–	–	176.71

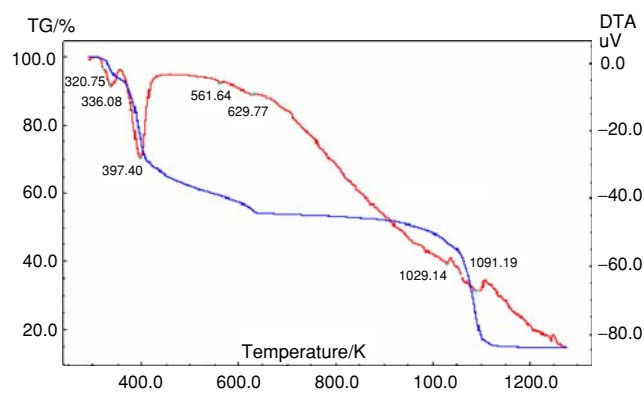
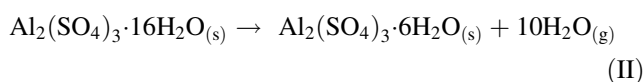
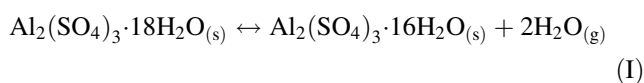


**Fig. 1** TG and DTA curves of  $\text{Al}_2(\text{SO}_4)_3 \cdot 18\text{H}_2\text{O}$  in  $4\text{ }^\circ\text{C min}^{-1}$

The reaction activation energy values are calculated using the Ozawa, KAS, Isoconversional and Friedman methods for all stages and for the values of decomposition ratios  $\alpha$  varying from 0.05 to 1.00. The calculated values for the activation energies of the dehydration reaction at Stage-I with respect to the decomposition ratio are presented in Fig. 2a.

It is observed that the activation energy values, which are calculated using these four methods, correlate with each other and result with an average value of  $36.23\text{ kJ mol}^{-1}$ . It is also found that, the variations of activation energy values with respect to the decomposition ratio are similar. The activation energy decreases with an increase in decomposition ratio, and it reaches to a minimum value for decomposition ratio ranging in between 0.45 and 0.55. After reaching to the minimum value, the activation energy increases with the increase in decomposition ratio.

Since there is not any available information on the compound- $\text{Al}_2(\text{SO}_4)_3 \cdot 16\text{H}_2\text{O}$ , which is the product of dehydration reaction for the Stage-I, it is supposed that this compound forms at reaction stage and is not stable at ambient conditions. In other words, it is found that the dehydration reaction at Stage-I is reversible.



The endothermic peak of dehydration reaction for the Stage-II is obvious in curves for all heating rates and more limited variation is observed for the peak temperature with respect to the heating rate. This reaction occurs at a temperature range of 354–458 K and approximately at peak temperature value of 400.6 K. It is found that the calculated value of dehydration enthalpy at lower heating rate is close to the dehydration enthalpy of the Stage-I and is  $74.64\text{ kJ mol}^{-1}\text{water}^{-1}$ .

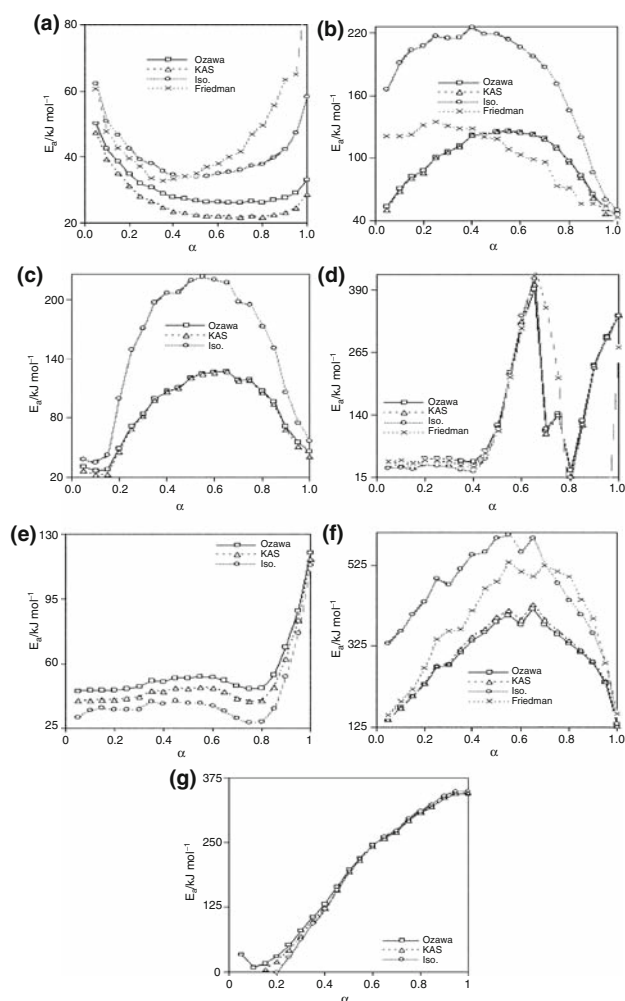
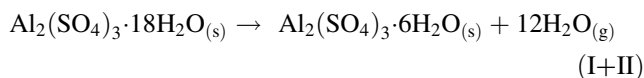


**Fig. 2** Variation of activation energy values with decomposition ratio  $\alpha$ , **a** major reaction step I, **b** major reaction step II, **c** reaction step I + II (combined step), **d** major reaction step III, **e** sub-stage IIIa, **f** sub-stage IIIb, **g** sub-stage IIIc

The activation energy values of dehydration reaction at Stage-II are calculated by using these four different methods and the variation with respect to decomposition ratio  $\alpha$  is plotted in Fig. 2b. While calculating the activation energy, the Ozawa and KAS methods provide perfectly compatible results, however, the value of activation energy obtained by using Isoconversional method is found to be approximately the twice of the value calculated by using these two models. Activation energy values calculated by Friedman's method may deviate from the activation energy values calculated by the other methods. This is due to the fact that Friedman's method is based on differential unlike the others use integrals. The decomposition ratio  $\alpha$  dependence of activation energy values determined by first three methods show similar tendencies. They all increase with an increase in decomposition ratio, reach to a maximum for decomposition ratio values in between 0.50

and 0.55. After reaching to the maximum, the values of activation energy decrease gradually. The average value of activation energy that is obtained by using these four methods, is  $117.03 \text{ kJ mol}^{-1}$ , which is higher than three times the average value for the Stage-I.

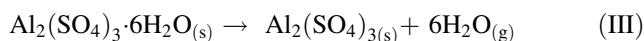
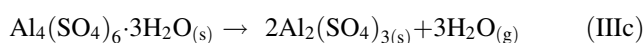
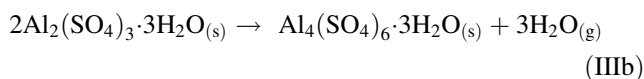
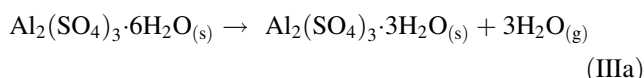
The variation of calculated activation energy for this combined dehydration reaction with respect to the decomposition ratio is plotted in Fig. 2c.



It is more appropriate supposing that dehydration reactions at Stage-I and II as a single reaction with regard to the stable aluminum sulfate compounds. The calculated enthalpy of dehydration reaction, if two stages are supposed as a single stage, does not vary with respect to the heating rate  $\beta$ , and results in an average value of  $84.23 \text{ kJ mol}^{-1} \text{ water}^{-1}$ .

While calculating the activation energy, the Ozawa and KAS methods provide perfectly compatible results with each other, however, using the Isoconversional method results in 80% larger values than these two methods. It is observed that, the variation of calculated activation energy with respect to the decomposition ratio is similar. At the beginning, the variation slightly decreases then tends to increase with the increase in decomposition ratio with reaching a maximum value in the range of 0.55–0.65. After reaching to the maximum value, the activation energy gradually decreases with the increase in decomposition ratio. The average value of activation energy that is calculated by using three methods, averages a values of  $106.12 \text{ kJ mol}^{-1}$ , which is slightly lower than the average value of Stage-II.

As a result of dehydration reaction at Stage-II (or combined step),  $\text{Al}_2(\text{SO}_4)_3 \cdot 6\text{H}_2\text{O}$ , which is a stable hydrate salt, forms. At Stage-III, the dehydration reaction of  $\text{Al}_2(\text{SO}_4)_3 \cdot 6\text{H}_2\text{O}$  occurs at three sub-stages (Fig. 1; Table 1).



During the first sub-stage of dehydration at Stage-III, three moles of water leaves the compound gradually, so active endothermic properties are not observed. The water that leaves the compound is observed such a continuation of the water molecules that left the compound at Stage-II.

A sub-product,  $\text{Al}_2(\text{SO}_4)_3 \cdot 3\text{H}_2\text{O}$ , forms with the leave of three moles of water from the compound  $\text{Al}_2(\text{SO}_4)_3 \cdot 6\text{H}_2\text{O}$ . The endothermic decomposition of this sub-product is obvious in all three heating rates resulting with a closer peak temperature values for all three heating rates, which has a value of 630 K. The first half of departing water molecules leaves the compound (IIIb) in a narrow temperature range (approximately  $60 \text{ }^\circ\text{C}$ ), while other half leave the compound (IIIc) slowly in a wide temperature range (approximately  $330 \text{ }^\circ\text{C}$ ) to form dehydrated aluminum sulfate. The anhydrous  $\text{Al}_2(\text{SO}_4)_3$  arises at 980 K at the end of these sub-stage.

Hence the endothermic peak areas are too small to measure during dehydration reaction of  $\text{Al}_2(\text{SO}_4)_3 \cdot 6\text{H}_2\text{O}$ , reaction enthalpy values for major and sub stages are not able to be calculated. The values of activation energy for the dehydration reaction at Stage-III that is calculated by using four methods and its variation with respect to the decomposition ratio are plotted in Fig. 2d. Hence lower  $r^2$  values are obtained in regression analysis of the Stage-III when compared with to those of first and second dehydration step; the existence of different regions in activation energy  $\alpha$  graph enforced us to evaluate the third dehydration step in three sub-stages.

The activation energy values of each sub-stages, IIIa, IIIb, and IIIc, calculated by using different methods and their variation behavior with respect to the decomposition ratio are presented in Fig. 2e–g, respectively. The value of the average activation energy and the tendency in the variation of the activation energy with respect to the decomposition ratio prove that dehydration occurs with different mechanisms in each sub-stage. The activation energy values are nearly constant, which require lower activation energy, during the most of the sub-stage IIIa and starts rapidly increase by the end of this stage. The tendency in the increase of the activation energy continues till to the half of the sub-stage IIIb. The findings from thermal analysis and activation energy presents that dehydration in the sub-stage IIIb is quite different than the dehydration at other sub-stages.

The average activation energy values calculated by using Ozawa, KAS, Isoconversional methods are 49.20, 350.66, and  $199.04 \text{ kJ mol}^{-1}$  for dehydration reactions at sub-stages IIIa, IIIb, and IIIc, respectively. The differences of activation energy values prove that dehydration reaction takes place in different sub-stages with different mechanisms.

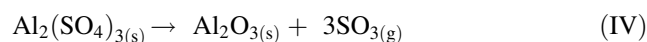
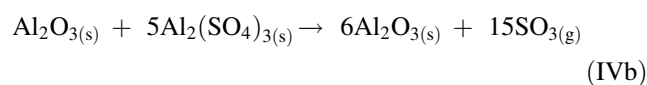
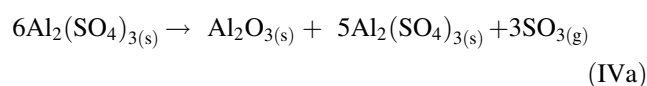
Findings of the thermal analysis and activation energy do not provide complete information to identify the exact temperature, at which the dehydrated aluminum sulfate formed.

Thermal decomposition of the dehydrated aluminum sulfate, which was formed as a product of dehydration

reaction, presents splitting-up with a loss of mass, which is equivalent to 0.50 moles of  $\text{SO}_3$  at 965–1050 K temperature range, at lower heating rates. Although an endothermic peak of the reaction is observed with the first two heating rates, the same peak is not observed with the highest heating rate (Fig. 1; Table 1).

As pointed out in the literature, it is identified that the actual decomposition of the dehydrated aluminum sulfate starts after a temperature of 1043 K, with an average peak temperature value of 1100 K. Although the majority (2.25 moles) of the gas product, which forms due to decomposition, leaves the compound at 1043–1120 K temperature range, the loss of mass continued until approximately 1150 K at all heating rates.

It is found that reaction enthalpy values, which are calculated using the endothermic peak areas belongs to the decomposition of aluminum sulfate, decreases with the increase in the heating rate, and has a value of 82 kJ per mol of produced  $\text{SO}_3$ , or an approximate value of 172.85 kJ per mol of the decomposed compound.



The activation energy values for the thermal decomposition reaction of the dehydrated aluminum sulfate, which is defined with the equation IV, are calculated by using all three methods. However, due to extreme deviation and less reliability by Friedman method, the values by Friedman method is not used. The variation graph is also presented by Fig. 3a.

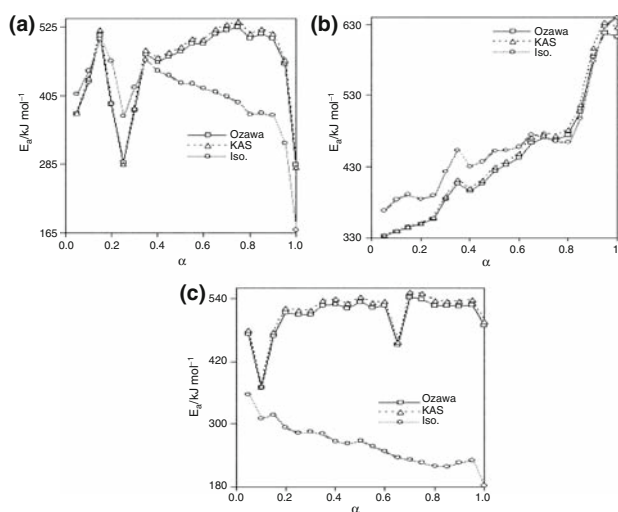


**Fig. 3** Variation of activation energy values with decomposition ratio  $\alpha$  **a** major reaction step IV, **b** sub-stage IVa, **c** sub-stage IVb

**Table 2** Average activation energies of all major steps with respect to applied methods and general average activation energy value

Reactions	I	II	III	IV
$T_{\text{peak}}/\text{K}$	354.17	400.57	630.45	1100.85
% Mass loss (Theo.)	5.407	27.033	16.220	36.041
% Mass loss (exp.)	5.410	27.058	16.240	34.828
Average $E_a/\text{kJ mol}^{-1}$				
Ozawa	30.77	96.41	139.12	454.84
KAS	26.57	94.75	135.67	460.46
Isoconversional	41.09	175.87	133.96	403.21
Friedman	46.47	101.09	146.25	–
Generally average	36.23	117.03	138.75	439.50

The activation energy values of major decomposition step IV determined by three methods compete with each other well and give us an average activation energy value, 439.50  $\text{kJ mol}^{-1}$ . This value is higher than the values of dehydration reactions for all major and sub-stages comparatively. Average activation energies of all major steps with respect to applied methods and general average activation energy value are summarized in Table 2.

The values of thermal analysis and activation energies, and variation graphs points out that decomposition of sulfate occurs in two different sub-stages. For this reason, activation energy values are calculated for each reaction, which are defined with IVa and IVb. The variation graphs for the activation energy with respect to the decomposition ratio are presented with Fig. 3b and c, respectively.

The average of activation energy values calculated by using three methods, which are compatible with each other, for the reaction IVa is 449.81  $\text{kJ mol}^{-1}$ . It is observed that, the variation of activation energy with respect to the decomposition ratio is also similar, which persistently increases with the increase in decomposition ratio and reaches at the end to the twice of the value at the beginning of the reaction.

Although the activation energy values of the reaction IVb calculated by using the Ozawa and KAS methods shows perfect compatibility with each other, the values calculated by using Isoconversional method quite differs from values by other two models. The variation of activation energy calculated by using the Ozawa and KAS methods with respect to the decomposition ratio are similar, which reaches a minimum in decomposition ratio values of 0.10 and 0.65 and are approximately constant for other values. On the other hand, the variation of activation energy calculated by using the Isoconversional method persistently decreases with the increase in the decomposition ratio. The average activation energy value, which is 260.31  $\text{kJ mol}^{-1}$  calculated by using Isoconversional method is almost half of the average value, which is 510.60  $\text{kJ mol}^{-1}$ , calculated by using other two models.

## Conclusions

Thermal decomposition of the  $\text{Al}_2(\text{SO}_4)_3 \cdot 18\text{H}_2\text{O}$  was studied TG method. It is found that the compound decomposes in four major stages. Three dehydration and a sulfate decomposition reaction stages were investigated in a detailed way. The activation energies of the decompositions were calculated by using the model free equations; the Ozawa, KAS, Isoconversional. Hence it is based on differential formulation, the Friedman method may deviate from other methods, which are based on integral formulation, while calculating the activation energy.

The activation energy values of the dehydration reaction at first Stage-I decrease with an increase in decomposition ratio  $\alpha$  up to 0.55, then the activation energy values continuously increase. In contrast to Stage-I, the activation energy values of dehydration reaction at Stage-II and IIIb increase with an increase in decomposition ratio  $\alpha$  up to 0.55 and then decrease with decreasing  $\alpha$  continuously referring to a nucleation and growth kinetic mechanism.

Although the differentiation in between decomposition enthalpy of sulfate ( $82 \text{ kJ mol}^{-1}$ ) and the dehydration enthalpies of Stage's I, II and (I+II) (73, 75, and  $84 \text{ kJ mol}^{-1}$ , respectively) is very limited, it is observed that there is an effective differentiation in between activation energies of reactions. The average of activation energy values, which increase with the decrease in the amount of hydrate water in the compound, for dehydration reactions at Stage-I, II, and IIIb are 36, 117, and  $358 \text{ kJ mol}^{-1}$ , respectively. At decomposition ratio ( $\alpha$ ) value of 0.55, at which the nucleation is completed, the average values of activation energy for reactions at Stage-II and IIIb ( $157$  and  $471 \text{ kJ mol}^{-1}$ , respectively) reach to the maximum value within the series.

As expected, it is observed that the activation energy values that belong to the decomposition of sulfate are always higher than the activation energy values of dehydration reaction. A continuous increase of the activation energy until the end of first decomposition step ( $630 \text{ kJ mol}^{-1}$ ) observed and followed by fluctuations with  $500 \text{ kJ mol}^{-1}$  of activation energy value for the whole sulfate decomposition reaction.

## References

- Croix A, English RB, Brown ME, Glasser L. Modeling the thermal decomposition of solids on the basis of lattice energy changes. Part I: alkaline-earth carbonates. *J Solid State Chem.* 1998;137:332–45.
- Liu Y, Zhao J, Zhang H, Zhu Y, Wang Z. Thermal decomposition of basic zinc carbonate in nitrogen atmosphere. *Thermochim Acta.* 2004;414:121–5.
- Valdiviseo F, Boineau V, Pijolat M, Soustelle M. Kinetic study of the dehydration of lithium sulphate monohydrate. *Solid State Ion.* 1997;101–103:1299–303.
- Huuska M, Koskenlinna M, Ninisto L. Thermal decomposition of iron sulphates: I. Thermogravimetric study of  $\text{FeSO}_4 \cdot \text{H}_2\text{O}$  in carbon monoxide and hydrogen atmospheres. *Thermochim Acta.* 1975;13:315–20.
- Pacewska B, Pysiak J, Klepanska A. The investigations of thermal decomposition process of basic aluminium potassium sulfate in the reduced conditions. *Thermochim Acta.* 1985;92:657–9.
- Straszko J, Humienik MO, Mozejko J. Kinetics of thermal decomposition of  $\text{ZnSO}_4 \cdot 7\text{H}_2\text{O}$ . *Thermochim Acta.* 1997;292:145–50.
- Chou K-S, Soong C-S. Kinetics of multistage dehydration of aluminum sulfate hydrate. *Thermochim Acta.* 1984;81:305–10.
- Chou K-S, Soong C-S. Kinetics of thermal decomposition of aluminum sulfate. *Thermochim Acta.* 1984;78:285–95.
- Madarász J, Pokol G, Gal S. Application of non-linear regression methods for the estimation of common kinetic parameters from several thermoanalytical curves. *J Therm Anal Calorim.* 1994;42:539–50.
- Lapides IL. Evaluation of kinetic parameters from a single TG curve based on the similarity theory and process symmetry. *J Therm Anal Calorim.* 1997;50:269–77.
- Ozawa T. Kinetic analysis of derivative curves in thermal analysis. *J Therm Anal Calorim.* 1970;2:301–24.
- Gabal MA. Non-isothermal studies for the decomposition course of  $\text{CdC}_2\text{O}_4\text{-ZnC}_2\text{O}_4$  mixture in air. *Thermochim Acta.* 2004;412:55–62.
- Küçük F, Yıldız K. The decomposition kinetics of mechanically activated alunite ore in air atmosphere by thermogravimetry. *Thermochim Acta.* 2006;48:107–10.
- Chuanming L, Donghua C, Wanjun T, Yuhua P. Synthesis of  $\text{MgNi}_2\text{O}_3$  and kinetics of thermal decomposition of the oxalate precursor. *J Anal Appl Pyrolysis.* 2006;75:240–4.
- Su TT, Jiang H, Gong H. Thermal decomposition and dehydration kinetic studies on hydrated  $\text{Co(II) methanesulfonate}$ . *Thermochim Acta.* 2005;435:1–5.
- Ammar K, Flanagan DR. Role of isoconversional methods in varying activation energies of solid-state kinetics I. Isothermal kinetic studies. *Thermochim Acta.* 2005;429:93–102.
- Liu Y, Mab B, Zhao X, Deng Y, Zhang H, Wang Z. The decomposition of  $\text{Co(NIA)}_2(\text{H}_2\text{O})_4$  in nitrogen atmosphere. *Thermochim Acta.* 2005;433:170–2.
- Wang J, Laborie MG, Wolcott MP. Comparison of model-free kinetic methods for modeling the cure kinetics of commercial phenol–formaldehyde resins. *Thermochim Acta.* 2005;439:68–73.
- Doğan F, Kaya I, Yürekli M. Kinetic of thermal degradation of poly(isobornyl methacrylate). *Catal Lett.* 2007;114(1–2):49–54.
- Criado JM, Sánchez-Jiménez PE, Pérez-Maqueda LA. Critical study of the isoconversional methods of kinetic analysis. *J Therm Anal Calorim.* 2008;92(I):199–203.
- Wang S-X, Tan Z-C, Li Y-S, Sun L-X, Li Y. Kinetic analysis of thermal decomposition of polyaniline/ $\text{ZrO}_2$  composite. *J Therm Anal Calorim.* 2008;92(II):483–7.
- Dias DS, Crespi MS, Ribeiro CA, Fernandes JLS, Cerqueira HMG. Application of non-isothermal cure kinetics on the interaction of poly(ethylene terephthalate)-alkyd resin paints. *J Therm Anal Calorim.* 2008;91(II):409–12.
- Vlase T, Vlase G, Birta N, Doca N. Comparative results of kinetic data obtained with different methods for complex decomposition steps. *J Therm Anal Calorim.* 2007;88(III):631–5.